

## VACUUM ISSUES OF SIS18 UPGRADE AT GSI\*

H. Kollmus, M.C. Bellachioma, M. Bender, A. Krämer, J. Kurdal, H. Reich-Sprenger  
GSI-Darmstadt, Germany

### Abstract

The FAIR project “Facility for Antiproton and Ion Research” at GSI is designed to deliver heavy ion beams of increased energy at highest luminosity. The gain in energy compared to the existing facility will be about a factor of 15, while the gain in intensity is planned to be in the range of up to a factor of 1,000 for primary beams and up to a factor of 10,000 for secondary beams. The existing GSI facility including the heavy ion synchrotron SIS18 will act as injector for the FAIR accelerator complex. The higher intensities compared to the present situation will be realized by a faster cycling time and, for heavy ions, lower charge state which enters quadratically into the space charge limit. However, the lower charge state, e.g.  $U^{28+}$ , leads to an enhanced ionization cross section compared to high charge states. The design-value for SIS18 is to deliver  $10^{12}$   $U^{28+}$  ions per second in a 4 Hertz operation mode [1]. To minimize beam loss by charge exchange a dynamic vacuum (vacuum during beam operation) in the  $10^{-12}$  mbar region –with a low fraction of heavy residual gas components– is required. At the moment SIS18 has a static pressure of about  $10^{-11}$  mbar, but during operation local pressure rises were observed due to ion induced desorption limiting the ion beam life time. An intensive program to upgrade the vacuum system of SIS18 is in progress. Here, we will report on the three major tasks: ion induced desorption, new dipole and quadrupole chamber design and NEG coating.

### ION INDUCED DESORPTION

If highly energetic heavy ions in the vacuum system hit an aperture limiting device or the chamber wall, particles are released from the solid into the vacuum, measurable by a pressure increase. The number of released particles per incident ion, the so-called desorption yield, scales with the ion impact energy, the projectiles mass and atomic number and depends in addition on the projectile charge state and its angle of incident. Values of less than 1 up to 10,000 and more are reported for different collision systems [2, 3, 4]. To measure desorption yields for SIS18 relevant ions and energies, a dedicated test stand was built up. The experimental set-up consists of a UHV test chamber, equipped with an extractor ionization gauge and a quadrupole mass spectrometer, connected to the accelerator beam line by a conductance limiting vacuum tube and a set of differential pumping stages. Due to the conductance the pumping speed in the UHV test chamber is well defined. Differ-

ent targets can be adjusted onto the beam axis by a linear feedthrough. Details are described in [5]. The desorption yield  $\eta$  can be calculated from the total pressure increase  $\Delta p$  using the ideal gas law,

$$\eta = \frac{\Delta p \cdot S}{\dot{N} \cdot k \cdot T}$$

where  $S$  is the pumping speed,  $\dot{N}$  is the ion flux,  $k$  is the Boltzmann constant and  $T$  is the temperature. Recent desorption yield measurements for Ar and U ions at different impact energies are shown in Fig. 1 in comparison to their electronic energy loss inside of the target. At all impact

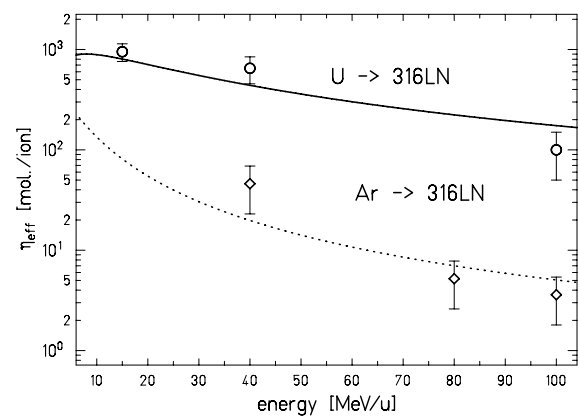


Figure 1: Desorption yields (points) and squared electronic energy loss (lines) versus impact energy for  $U^{73+}$  and  $Ar^{10+}$  hitting a stainless steel target. The electronic energy loss  $(dE/dx)^2$  is calculated using the CMEE library [6] and scaled to the measured values.

energies we are well above the Bragg-Peak maximum for both projectiles. One can clearly see, how the desorption yield is decreasing for increasing projectile energy, following roughly a  $(dE/dx)^2$  scaling. This scaling was proved for a given projectile ion at different energies but also for different ions at a given energy. A  $(dE/dx)^n$  scaling law is well known from sputter yield experiments with  $n$  ranging from 1-2:  $n=2$  hints to a thermal moderated process. This clearly shows that the ion induced desorption is linked to the electronic sputtering [7, 8]. In order to understand this in more detail an ERDA (Elastic Recoil ion Detection Analysis) set-up was taken into operation to characterize the targets *in-situ* during desorption yield measurements. A precise knowledge of the target properties (target impurities, oxide layer) is necessary to understand the desorption process [9]. The two major questions are: Is the ion induced desorption only a surface process, or are also impurities from the bulk of the material freed to the gas phase?

\* We acknowledge the support of the European Community-Research Infrastructure Action under the FP6 “Structuring the European Research Area” program (DIRACsecondary-Beams, contract number 515873)

How is the desorption yield influenced by surface properties, e.g. oxidation or roughness? A detailed description on the ERDA investigations can be found in the contribution to this conference by M. Bender.

## NEW DIPOLE AND QUADRUPOLE CHAMBERS FOR SIS18

The SIS18 with a circumference of 216 m is equipped with 24 dipole magnets, 12 triplet lenses and 12 sextupole lenses. Due to the high ramping rates – as injector for FAIR SIS18 will operate in 4 Hertz repetition mode – thin wall vacuum chambers are needed for all magnets to keep eddy currents at a tolerable level. Using stainless steel the maximum allowed wall thickness is 0.3 mm. The length of the dipole chambers is about 3 m with a bending angle of 15°. The straight quadrupole chambers are about 4 m long. Both chambers have an elliptical aperture and have to be bakeable to 250-300° C. To withstand the atmospheric pressure the thin walled vacuum chambers are supported by ribs parallel to the magnetic field lines. Presently the distance between two ribs is 10 mm. The chambers are heated by coaxial calorifier (heating pipes) limited to 150° C to avoid mechanical stress, which can cause leaks due to high temperature gradients during bake out. To go to higher bake out temperatures we have designed new dipole and quadrupole chambers. The material is again stainless steel with a thickness of 0.3 mm, but the distance between the supporting ribs is extended to 25 mm allowing to place heating jackets in between in direct contact to the thin walled chamber. In Fig. 2 one can see a picture



Figure 2: Photograph of the new dipole chamber with heating jackets.

of a part of the new dipole chamber. After mounting the heating stripes the whole chamber is wrapped with an isolation layer made from Kapton coated with an aluminum thin film, Microtherm plates and again Kapton foil. With this isolation the chambers can be heated up to 250° C extremely homogeneously and the temperature outside of the isolation keeps below 100° C to protect the surrounding magnet and to limit the required heating power. In Fig.

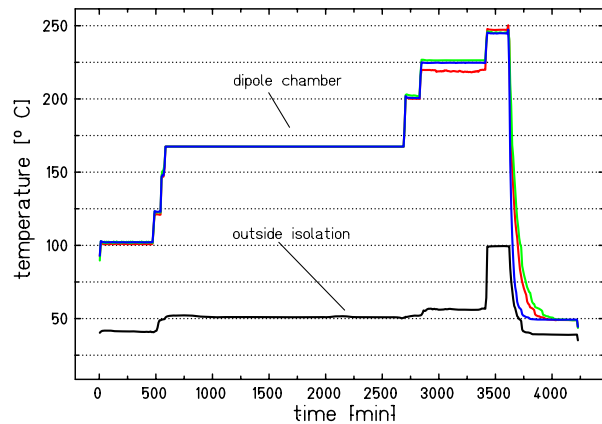


Figure 3: Temperature development during bake-out. Upper curves: temperature at different positions on the dipole chamber wall and the supporting ribs. Lower curve: temperature outside the isolation.

3 one example of the temperature evolution during bake-out is shown. The temperatures were measured at different positions of the dipole chamber: between two supports directly on the thin walled chamber (low heat capacity), on the supports (high heat capacity), and outside the isolation. A homogeneous temperature distribution is visible: There is no gradient between supporting ribs and the chamber itself. In addition the isolation seems to be sufficient: a bake-out temperature of 250° C was reached still not in full load operation.

Presently 26 new dipole chambers are built. The new heating jackets are evaluated and taken into operation. The first dipole chambers will be exchanged at the beginning in August 2006. New quadrupole chambers following the same design will be built in 2007 and most probably exchanged in 2008.

## NEG COATING AT GSI

As mentioned above, the dipole and the quadrupole chambers have a length of about 3 and 4 m resp. Due to their elliptical cross section of 190 mm x 70 mm for the dipole and 203 mm x 123 mm for the quadrupole chambers they have a limited conductance. Presently they are only pumped from outside since there is no access point for conventional pumping inside of the magnets. Distributed pumping via Non-Evaporable Getter thin films (NEG) is an excellent solution for conductance limited chambers like the dipole and quadrupole chambers in SIS18. For this purpose by the end of June 2005 a license agreement for the non evaporable thin film getters was signed between GSI and CERN and an activity was started at GSI with the aim of designing and commissioning a dipole chamber coating facility. Presently two NEG facilities are taken into operation at GSI. One dedicated for the coating of dipole chambers and a second one for the coating of chambers with a diameter of maximum DN 200 CF and a maximum length of 1 m. In Fig. 4 a photograph of the NEG coating facil-

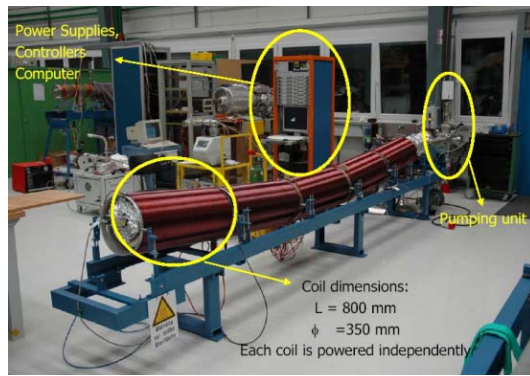


Figure 4: Picture of the NEG coating facility for SIS18 dipole chambers.

ity for the SIS18 dipole chambers is shown. The magnetic field of about 150 Gauss is realized by five individual powered coils. On one side the dipole chamber is connected to a pumping post and a gas inlet system. The pressure can be measured on both sides of the chamber. For a homogeneous coating two cathodes are used in the elliptical shaped dipole chamber placed approximately at the focus points of the elliptical cross section. During each coating a small

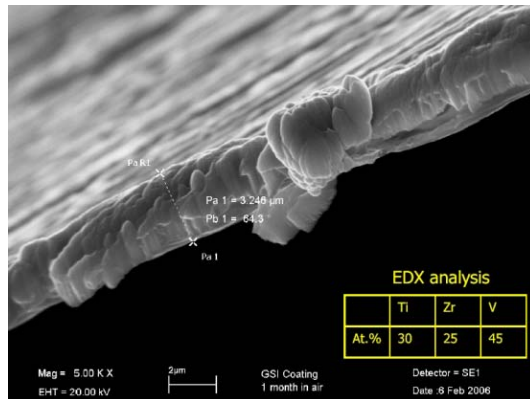


Figure 5: SEM Picture of the NEG film. Side view.

sample is mounted inside of the chamber for an easy offline analysis. The film characterization can be either performed by an ion beam analysis, e.g. ERDA (Elastic Recoil ion Detection Analysis), by XPS (X-ray Photoelectron Spectroscopy), by SEM (Scanning Electron Microscopy) or by EDX (Energy Dispersive X-ray analysis). As an example, the morphological analysis (performed by SEM) on the NEG thin film produced for the SIS18 quadrupole chamber is shown in Fig. 5. Additionally, the film stoichiometry was measured using the EDX technique also tabulated in Fig. 5. The pumping speed of the coated chambers is measured with a standard Fischer-Mommsen dome to be about  $7 \text{ l/s} \cdot \text{cm}^2$  for CO. The activation of the NEG film coating on the SIS18 dipole and quadrupole chambers will be realized using the new heating system. The activation temperature is about  $200^\circ \text{C}$ .

## CONCLUSION

In this work we have reported on three major tasks of the SIS18 vacuum upgrade with the goal to reach a pressure of  $10^{-12}$  mbar during high current beam operation. The tasks are either successfully done or in presentable progress:

- The origin of ion induced desorption is well understood by desorption yield and ERDA measurements. From the results we are able to propose low desorption materials for the SIS18 loss locations to minimize the pressure rises during high intensity operation to a tolerable level. Further investigations on coating techniques and diffusion barriers are in preparation. Details can be found in the contribution to this conference by M. Bender.
- New dipole chambers including bake out equipment are designed, manufactured and tested successfully. Quadrupole chambers will be build using the same concept.
- NEG coating technique is established at GSI with two NEG coating facilities. Several vacuum chambers have been already successfully coated and characterized, incl. 4 dipole chambers and one quadrupole chamber for the SIS18. The dipole chamber coating is in production mode.

Apart of these major tasks a few minor upgrade works will be done in the next year, e.g., the optimization of existing getter and titan sublimation pumps. The SIS18 UHV upgrade is scheduled to be complete in 2009.

## ACKNOWLEDGMENT

The desorption yield measurements were performed in a collaboration with E. Mahner (CERN). We would like to thank E. Mahner for technical support, discussion and help during beam time. In addition we would like to thank E. Hedlund, L. Westerberg and O. Malyshev for their help during the SIS18 beam times.

## REFERENCES

- [1] W. Henning, EPAC04 proceedings (2004)
- [2] E. Mahner et al., Phys. Rev. ST AB **6**, 013201 (2003)
- [3] E. Mahner et al., Phys. Rev. ST AB **7**, 013202 (2004)
- [4] A.W. Molvik et al., Phys. Rev. ST AB **7**, 093202 (2004)
- [5] H. Kollmus et al., AIP CP773 (2005) p. 207
- [6] Tech-X Corporation, www.txcorp.com
- [7] K. Wien, Radiation Effects and Defects in Solids, Vol. 109 (1989) p. 137-167
- [8] M. Toulemonde et al. NIM B 212 (2003) 346-357
- [9] H. Kollmus et al., GSI Scientific Report 2005